Cluster radioactivity:
exotic decay or dominant decay channel?

Michał Warda

Uniwersytet Marii Curie-Skłodowskiej
Lublin, Poland

Kraków, 15.11.2021

Collaboration:

- L.M. Robledo, UAM, Madrid
- A. Zdeb, UMCS, Lublin / CEA, Bruyères-le-Châtel

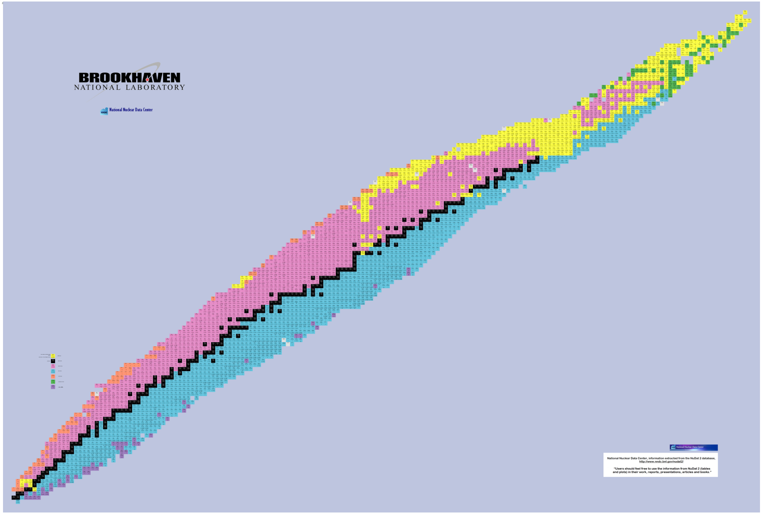
BROOKHAVEN
NATIONAL LABORATORY
National Nuclear Data Center
National Nuclear Data Center
National Nuclear Data Center, information extracted from the NuDat 2 database, http://www.nndc.bnl.gov/nudat2/
"Users should feel free to use the information from NuDat 2 (tables and plots) in their work, reports, presentations, articles and books."

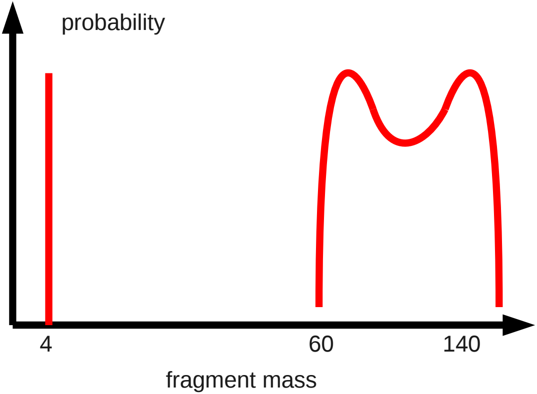
probability
4
60
140
fragment mass

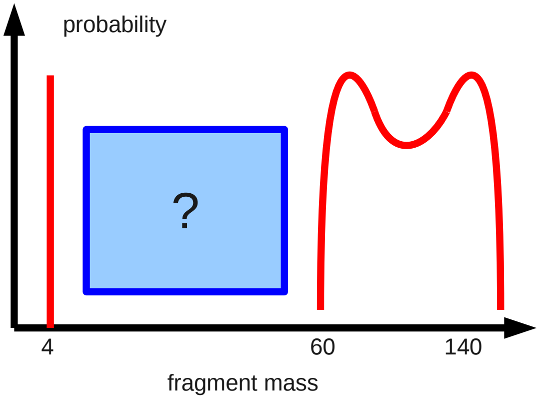
probability
?
4
60
140
fragment mass

Discovery of cluster radioactivity

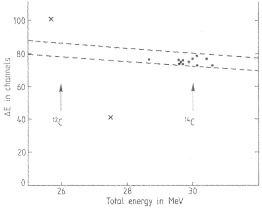

Fig. 1 Contents of the two-dimensional array ΔE versus E_{total} after a run of 189 days. The dotted line indicates the allowed region for carbon ions and the arrows indicate the total energies expected for ^{12}C and ^{14}C emissions in the decay of ^{223}Ra. The lower of the two crosses represents a quadruple pile-up. Below the total energy displayed, large numbers of triple and double α-pile-ups were recorded. Single α-events (and, in part, even double α-pile-ups) were biased out on the analogue side to avoid deadtime problems on the digital side. The upper cross is an event which was recorded during a thunderstorm which affected the mains badly. A run of 194 days was made before this one, yielding 8 events and, in addition, a run of approximately half a year was performed to investigate possible cosmic ray-induced events. Channel 77 in $\Delta E \approx 6.7$ MeV, which is exactly as expected for 30 MeV ^{14}C. Detector characteristics: The dead layer of the ΔE detector (200 mm^2 active area, 8.2 µm sensitive thickness) was determined to lie between 0.3 and 0.8 µm. In addition a protective layer of gold of thickness 20 µg cm^{-2} was evaporated on the source and 15 µg cm^{-2} carbon film inserted between the source and the ΔE detector. An extra 30–40 µg cm^{-2} of gold is present on the E-detector (300 mm^2 active area). This gives a total of 150–250 µg cm^{-2} of effective dead layer (Si equivalent) and an energy loss of ^{14}C ions of 0.5–0.8 MeV. The source of strength 3.3 µCi gave a counting rate of $\approx$4,000 s^{-1}, corresponding to an effective solid angle of detection of $\approx$1/3 sr.

$$^{223}_{88}\mathrm{Ra} \longrightarrow {}^{14}\mathrm{C} + {}^{209}\mathrm{Pb}$$

H.J. Rose and G.A. Jones, *Nature* **307**, 245 (1984)
Sandulescu, Poenaru and Greiner, *Sov. J. Part Nucl.* **11**, 528 (1980)

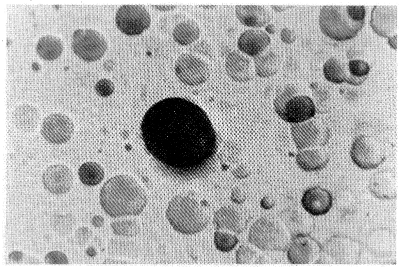

FIG. 1. Photomicrograph showing one etch pit due to a 56 MeV ^{24}Ne ion striking a Cronar detector nearly head on. About 3×10^6 alpha particles passed through this field of view.

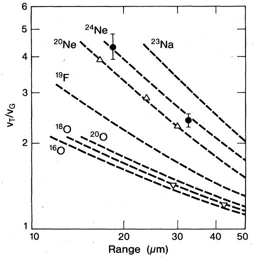

FIG. 2. Comparison of average signal of ^{24}Ne nuclei (●) emitted from ^{232}U with calibrations (dashed lines) obtained with ^{18}O (▽) and ^{20}Ne (Δ) ions at Lawrence Berkeley Laboratory accelerators. Ratio of etching rate along track to general etching rate v_T/v_G, is plotted as a function of residual range.

Barwick et al., PRC **31**, 1984 (1985)

UMCS

Cluster radioactivity: key facts

- Emitters: ${}^{221}_{87}$Fr — ${}^{242}_{96}$Cm
  12 even-even, 9 odd nuclei
- Clusters: ^{14}C — ^{34}Si
- Heavy mass residue: doubly magic ^{208}Pb ± 4 nucleons "Lead radioactivity"
- Half lives: 10^{11} s – 10^{26} s
- α branching ratio: 10^{-9} – 10^{-16}

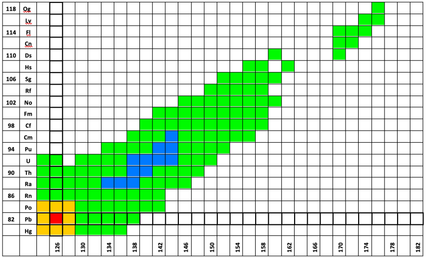

UMCS

Cluster radioactivity: key facts

- Emitters: ${}^{221}_{87}$Fr — ${}^{242}_{96}$Cm
  12 even-even, 9 odd nuclei
- Clusters: ^{14}C — ^{34}Si
- Heavy mass residue: doubly magic ^{208}Pb ± 4 nucleons "Lead radioactivity"
- Half lives: 10^{11} s – 10^{26} s
- α branching ratio: 10^{-9} – 10^{-16}

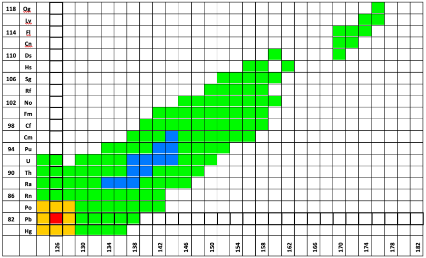

Cluster radioactivity: key facts

- Emitters: $^{221}_{87}$Fr — $^{242}_{96}$Cm
  12 even-even, 9 odd nuclei
- Clusters: ^{14}C — ^{34}Si
- Heavy mass residue: doubly magic ^{208}Pb ± 4 nucleons
  "Lead radioactivity"
- Half lives: 10^{11} s – 10^{26} s
- α branching ratio: 10^{-9} – 10^{-16}

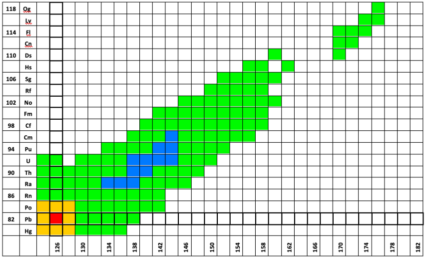

Cluster radioactivity: key facts

- Emitters: ${}^{221}_{87}$Fr — ${}^{242}_{96}$Cm
  12 even-even, 9 odd nuclei
- Clusters: ^{14}C — ^{34}Si
- Heavy mass residue: doubly magic ^{208}Pb ± 4 nucleons
  "Lead radioactivity"
- Half lives: 10^{11} s – 10^{26} s
- α branching ratio: 10^{-9} – 10^{-16}

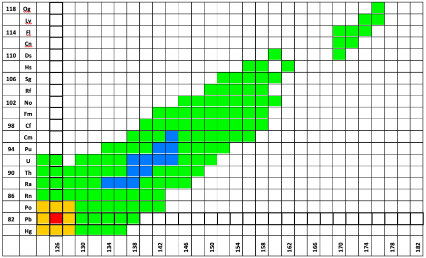

Cluster radioactivity: key facts

- Emitters: ${}^{221}_{87}$Fr — ${}^{242}_{96}$Cm
  12 even-even, 9 odd nuclei
- Clusters: ^{14}C — ^{34}Si
- Heavy mass residue: doubly magic ^{208}Pb ± 4 nucleons "Lead radioactivity"
- Half lives: 10^{11} s – 10^{26} s
- α branching ratio: 10^{-9} – 10^{-16}

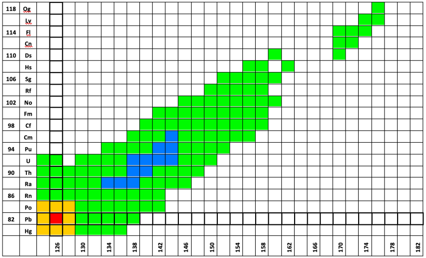

Theoretical description

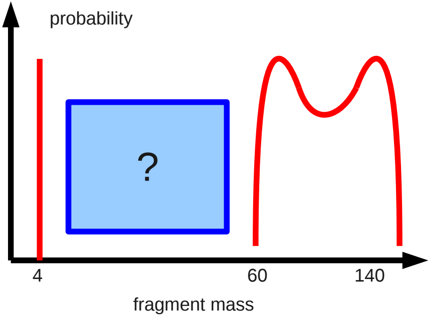

- Extrapolation of Gamov model of alpha emission
- Modified Geiger-Nuttall formula for half-lives
- Very asymmetric fission

Theoretical description

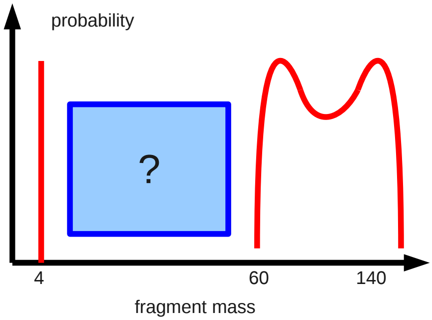

- Extrapolation of Gamov model of alpha emission
- Modified Geiger-Nuttall formula for half-lives
- Very asymmetric fission

Theoretical description

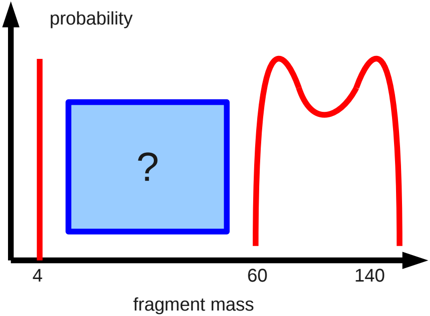

- Extrapolation of Gamov model of alpha emission
- Modified Geiger-Nuttall formula for half-lives
- Very asymmetric fission

Theoretical description

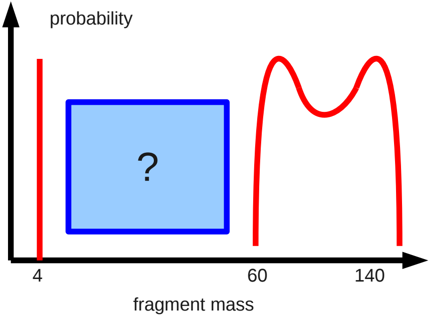

- Extrapolation of Gamov model of alpha emission
- Modified Geiger-Nuttall formula for half-lives
- Very asymmetric fission

Potential energy surface in fission

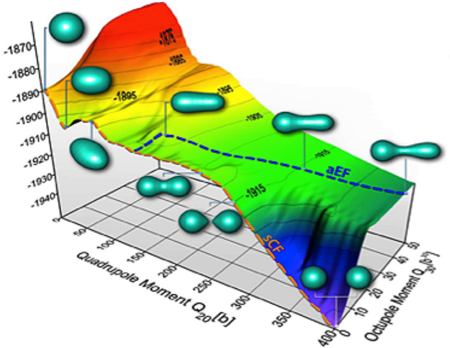

Figure by A. Staszczak

- Next slides show potential energy surfaces determined in the self-consistent method in HFB theory with Gogny D1S force

Potential energy surface in fission

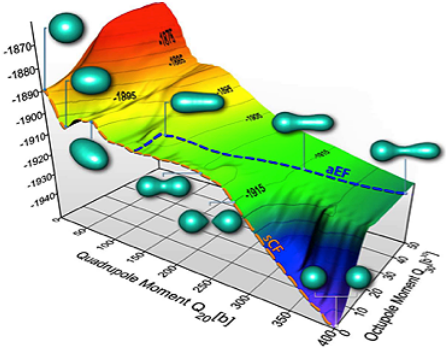

Figure by A. Staszczak

- Next slides show potential energy surfaces determined in the self-consistent method in HFB theory with Gogny D1S force

Shape evolution: ^{238}Pu

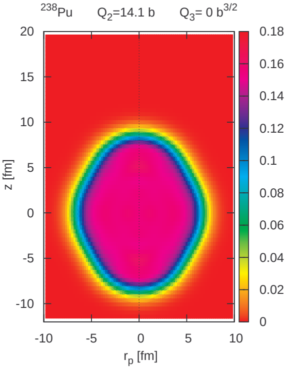

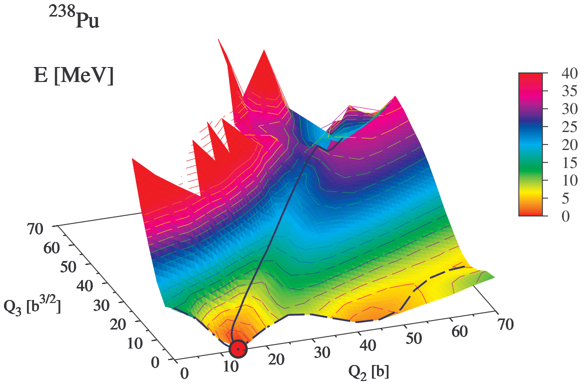

M. Warda and L. M. Robledo, Phys. Rev. C 84, 044608 (2011).

Shape evolution: ^{238}Pu

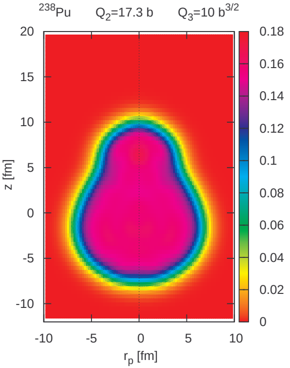

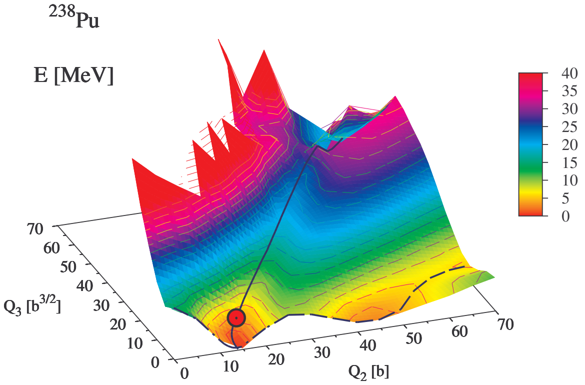

M. Warda and L. M. Robledo, Phys. Rev. C 84, 044608 (2011).

Shape evolution: ^{238}Pu

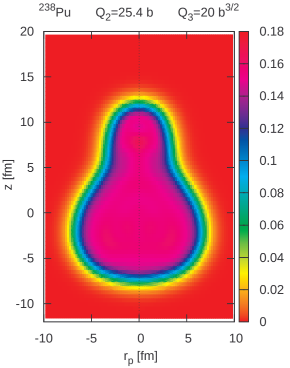

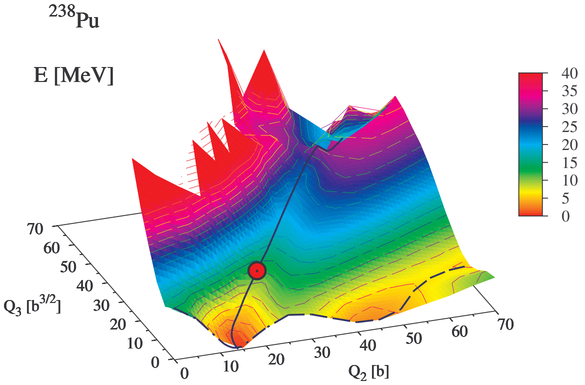

M. Warda and L. M. Robledo, Phys. Rev. C 84, 044608 (2011).

Shape evolution: ^{238}Pu

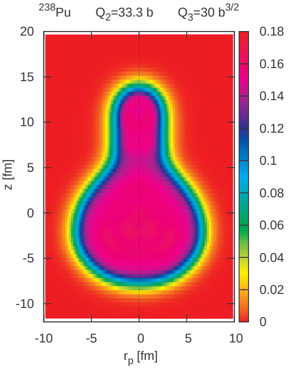

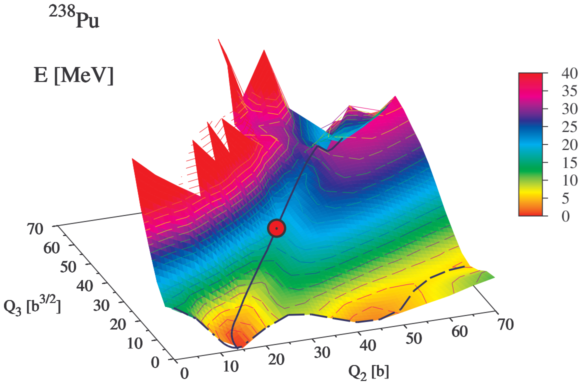

M. Warda and L. M. Robledo, Phys. Rev. C 84, 044608 (2011).

Shape evolution: ^{238}Pu

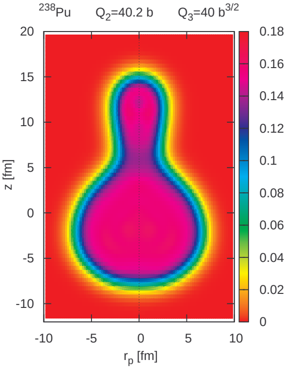

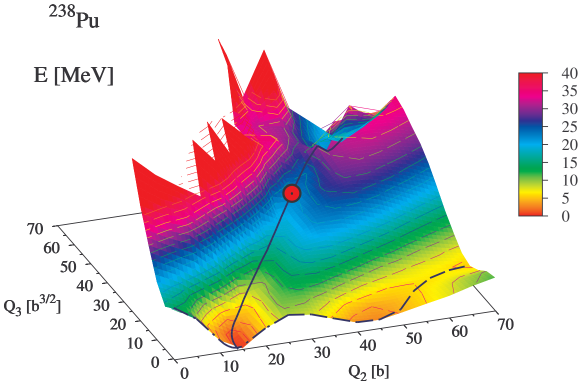

M. Warda and L. M. Robledo, Phys. Rev. C 84, 044608 (2011).

Shape evolution: ^{238}Pu

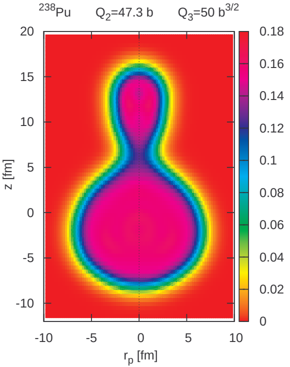

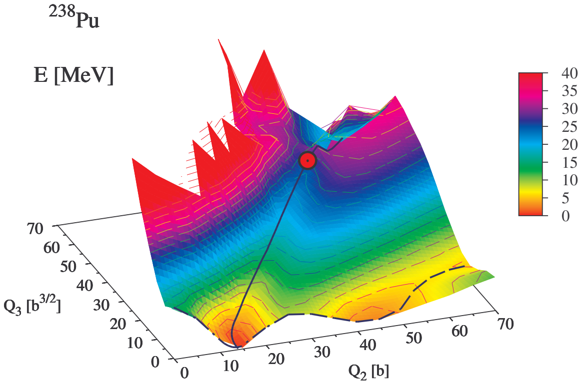

M. Warda and L. M. Robledo, Phys. Rev. C 84, 044608 (2011).

Shape evolution: ^{238}Pu

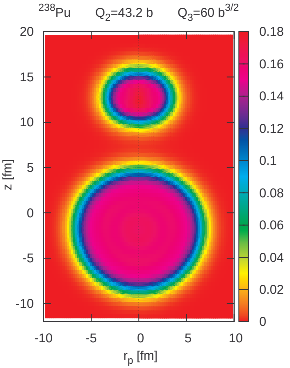

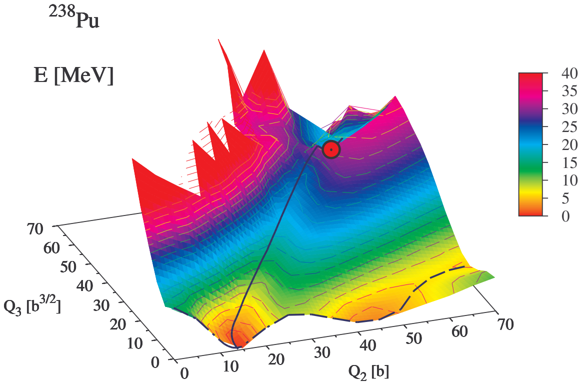

M. Warda and L. M. Robledo, Phys. Rev. C 84, 044608 (2011).

Shape evolution: ^{238}Pu

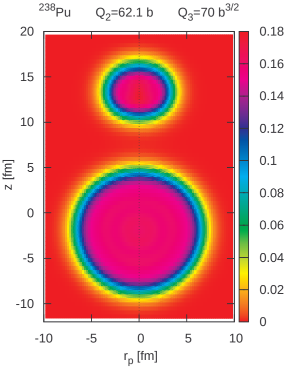

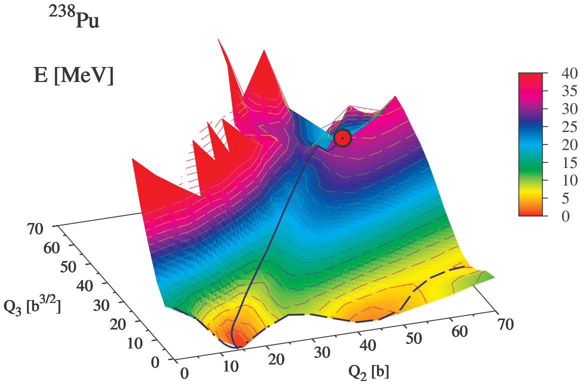

M. Warda and L. M. Robledo, Phys. Rev. C 84, 044608 (2011).

Shape evolution: ^{238}Pu

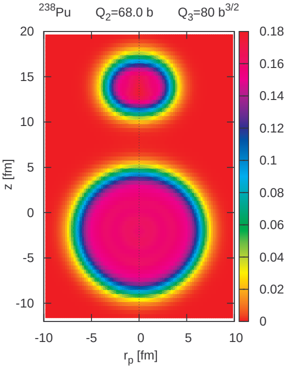

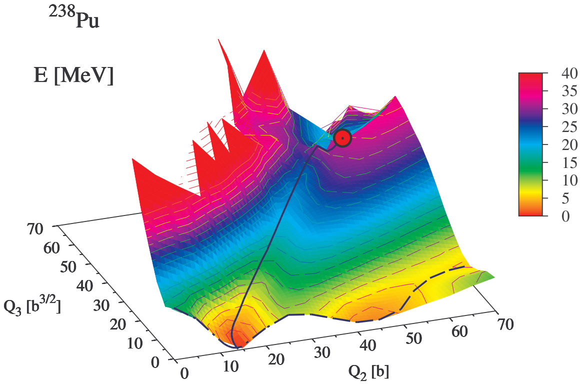

M. Warda and L. M. Robledo, Phys. Rev. C 84, 044608 (2011).

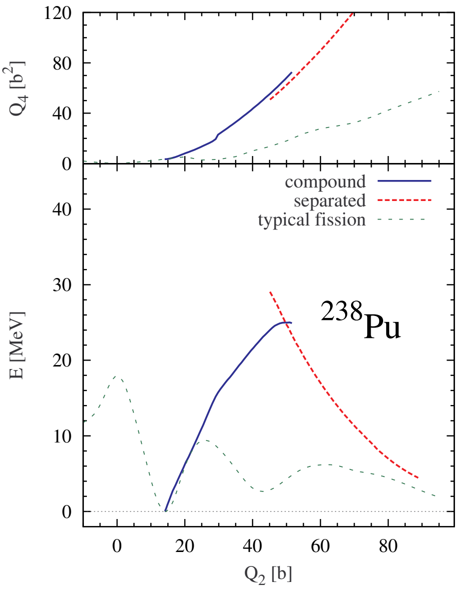

120
80
40
0
Q_4 [b^2]
compound
separated
typical fission
40
30
20
10
0
E [MeV]
^{238}Pu
0
20
40
60
80
Q_2 [b]

Half-lives

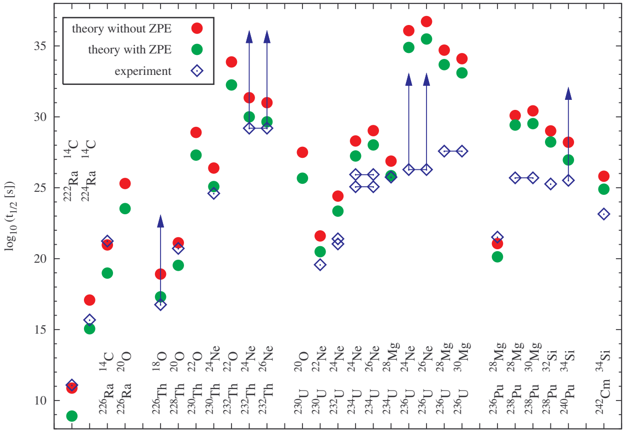
theory without ZPE
theory with ZPE
experiment
log10 (t1/2 [s])
10
15
20
25
30
35
222Ra 14C
224Ra 14C
226Ra 14C
226Ra 20O
226Th 18O
228Th 20O
230Th 22O
230Th 24Ne
232Th 22O
232Th 24Ne
232Th 26Ne
230U 20O
230U 22Ne
232U 24Ne
234U 24Ne
234U 26Ne
234U 28Mg
236U 24Ne
236U 26Ne
236U 28Mg
236U 30Mg
236Pu 28Mg
238Pu 28Mg
238Pu 30Mg
238Pu 32Si
240Pu 34Si
242Cm 34Si

Fission fragments - N/Z ratio

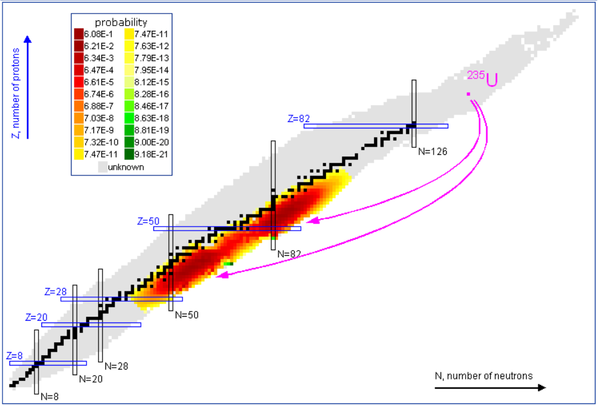

http://lablemminglounge.blogspot.com/2011/03/why-fuel-rods-are-radioactive.html

Fission fragments - N/Z ratio

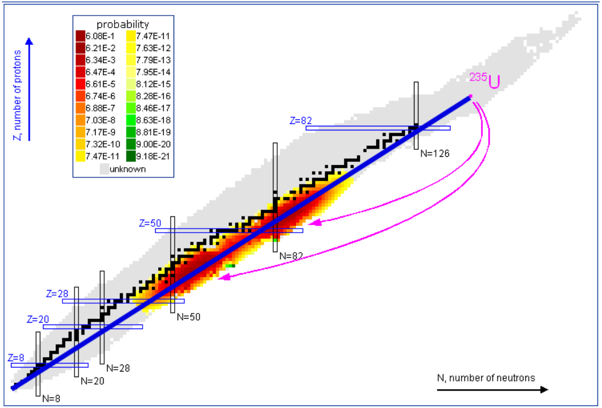

http://lablemminglounge.blogspot.com/2011/03/why-fuel-rods-are-radioactive.html

Cluster radioactivity - chart of nuclides

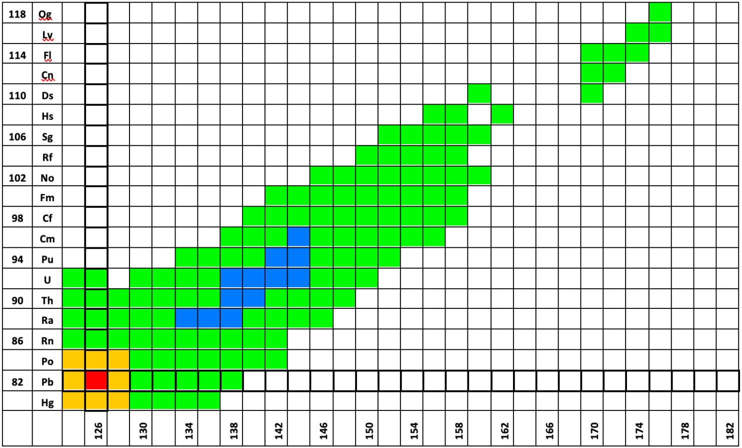

Cluster radioactivity - chart of nuclides

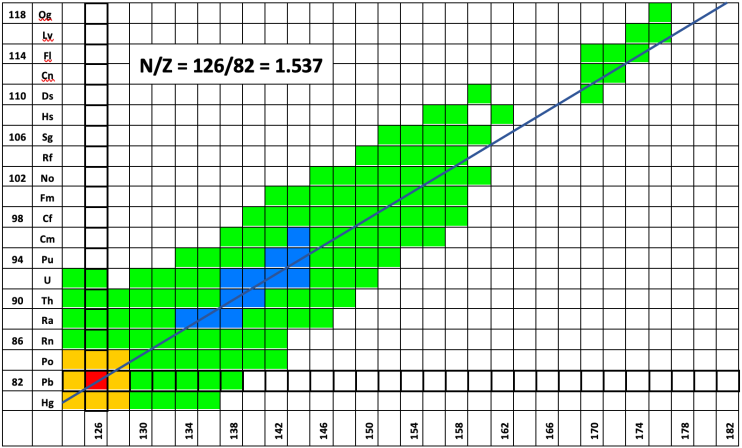

Cluster radioactivity - chart of nuclides

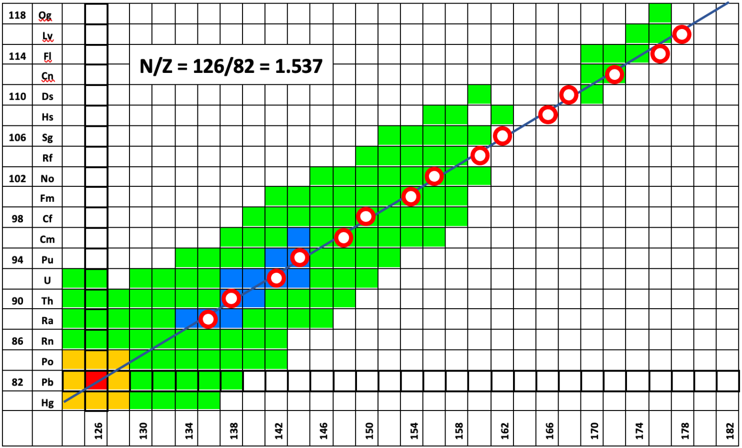

www.umcs.lublin.pl

Chart of SH nuclides

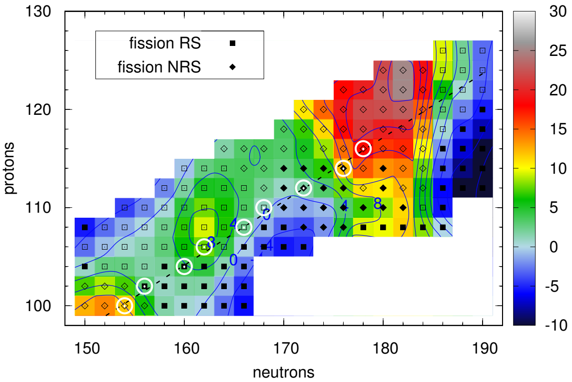

M. Warda, J.L. Egido, Phys. Rev. C 86 (2012) 014322
A. Baran, M. Kowal, P.G. Reinhard, L.M. Robledo, A. Staszczak, M. Warda, Nucl. Phys. A 944 (2015) 442

Fission barriers

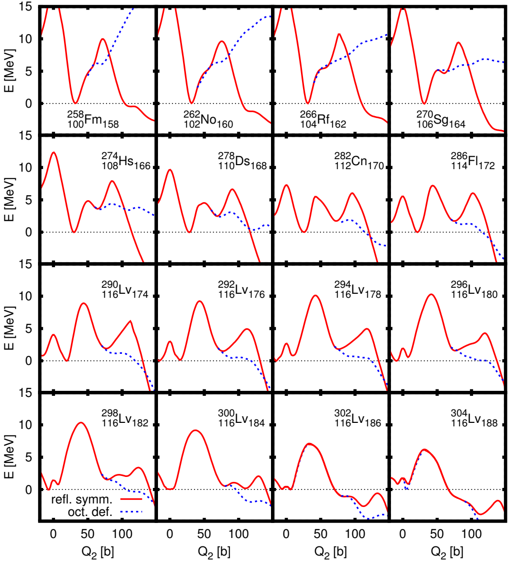

www.umcs.lublin.pl

Fission and α-decay half-lives

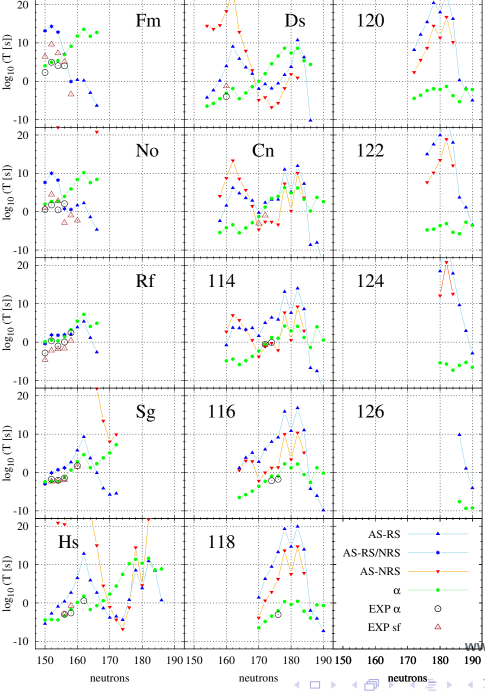

Previous approach

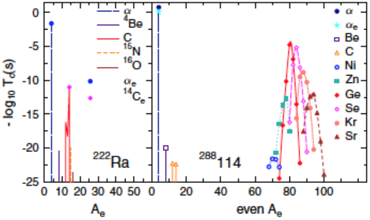

FIG. 1 (color online). Time spectra of different cluster emissions from ^{222}Ra (left panel) and from the superheavy nucleus ^{288}114 (right panel). The most probable emitted clusters from ^{222}Ra and ^{288}114 are ^{14}C and ^{80}Ge, respectively, both leading to ^{208}Pb daughter nucleus.

D. N. Poenaru, R. A. Gherghescu, and W. Greiner
Phys. Rev. Lett. 107, 062503 (2011); Phys. Rev. C 85, 034615 (2012)

Cluster radioactivity - chart of nuclides

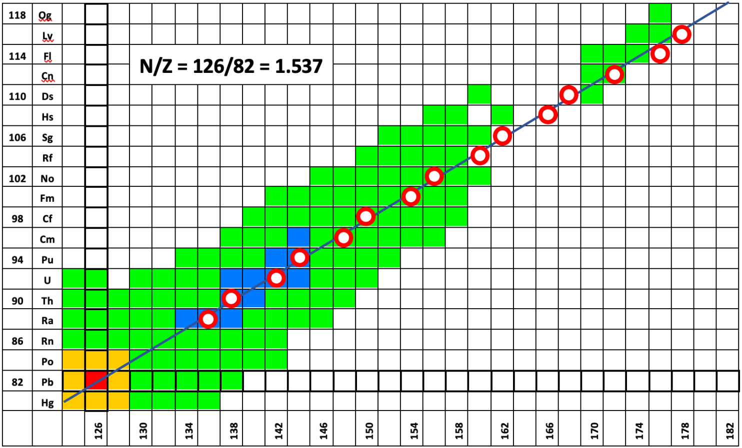

www.umcs.lublin.pl

^{224}Ra

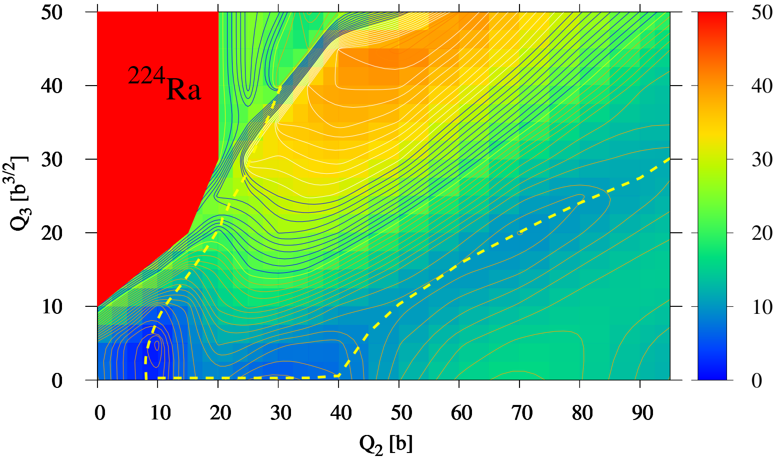

^{228}Th

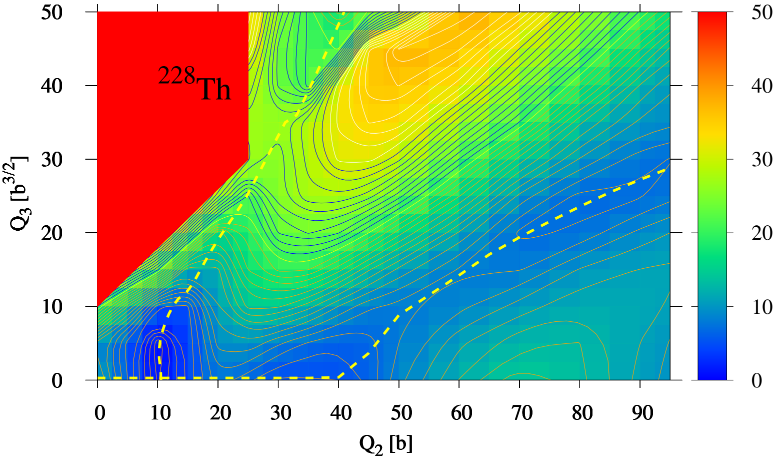

^{234}U

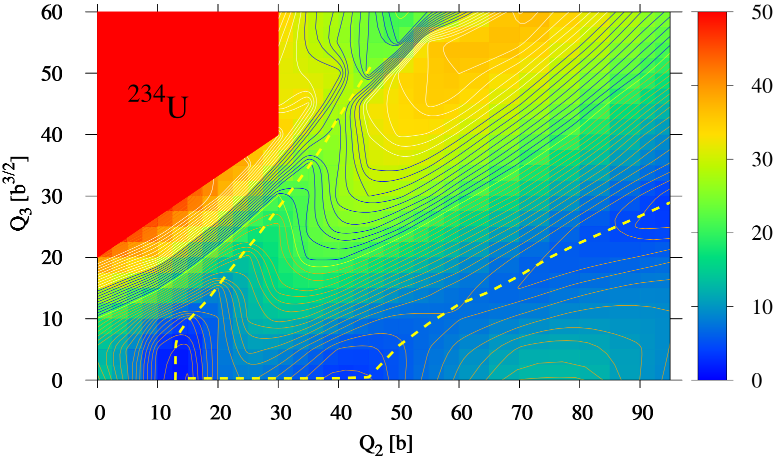

234U
60
50
40
30
20
10
0
Q3 [b3/2]
0
10
20
30
40
50
60
70
80
90
Q2 [b]
50
40
30
20
10
0

UMCS

^{238}Pu

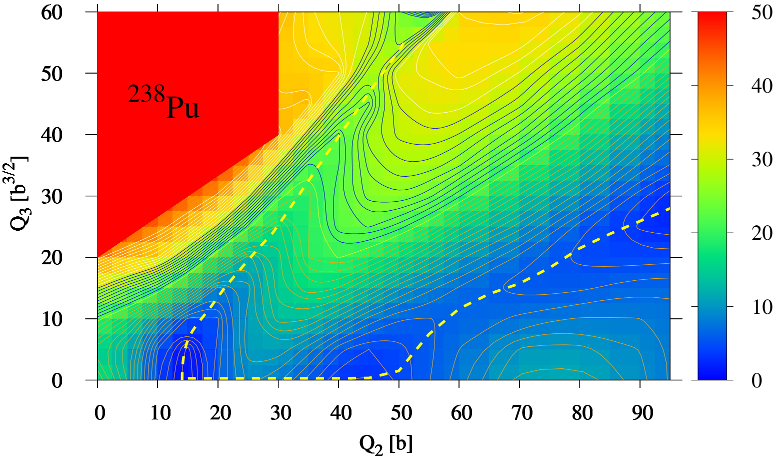

^{244}Cm

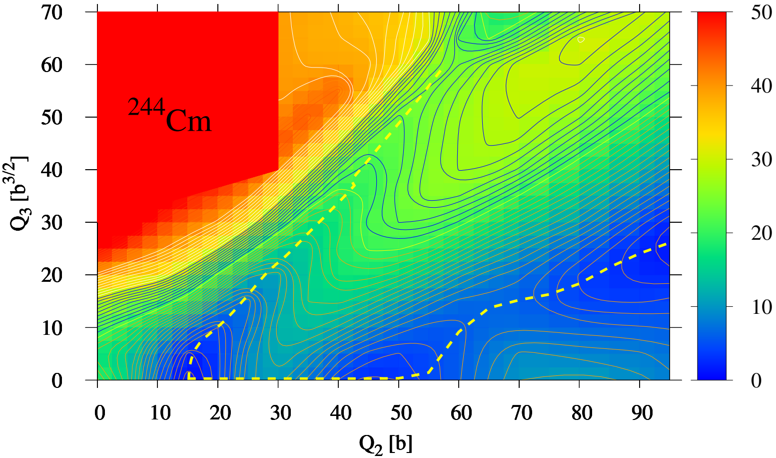
244Cm
Q3 [b3/2]
Q2 [b]
0
10
20
30
40
50
60
70
80
90
0
10
20
30
40
50
60
70
0
10
20
30
40
50

^{248}Cf

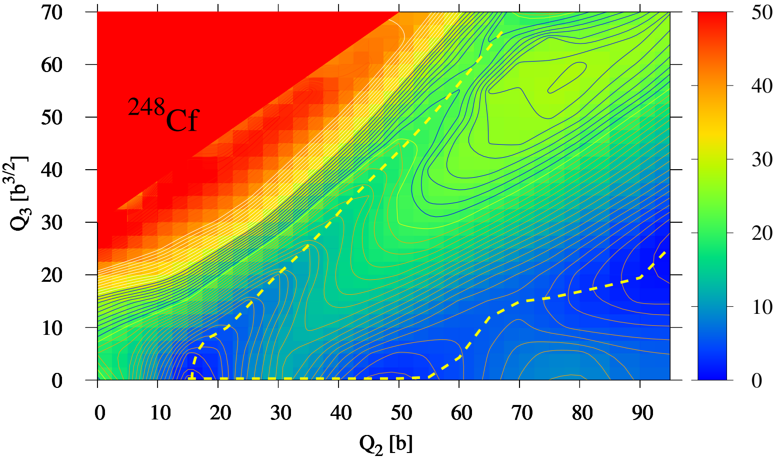

^{254}Fm

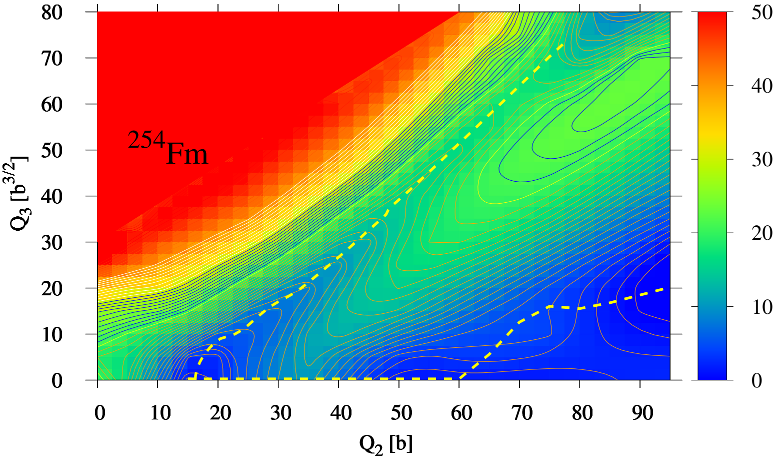

80
70
60
50
40
30
20
10
0
^{254}Fm
Q_3 [$b^{3/2}$]
0
10
20
30
40
50
60
70
80
90
Q_2 [b]
50
40
30
20
10
0

^{258}No

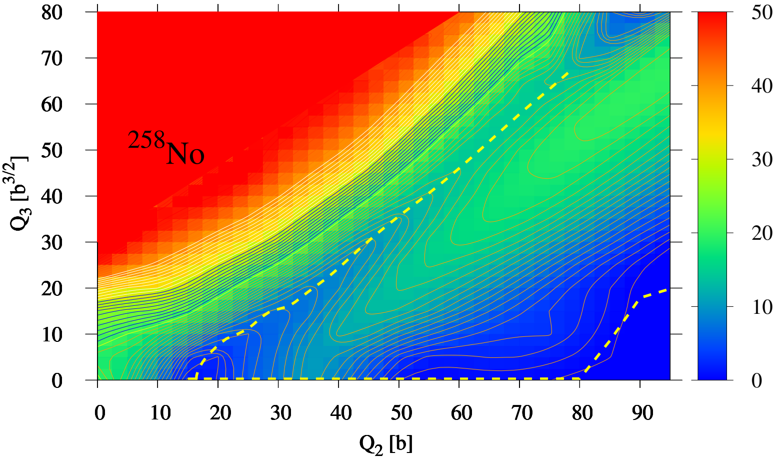

80
70
60
50
40
30
20
10
0
Q3 [b3/2]
258No
0
10
20
30
40
50
60
70
80
90
Q2 [b]
50
40
30
20
10
0

^{264}Rf

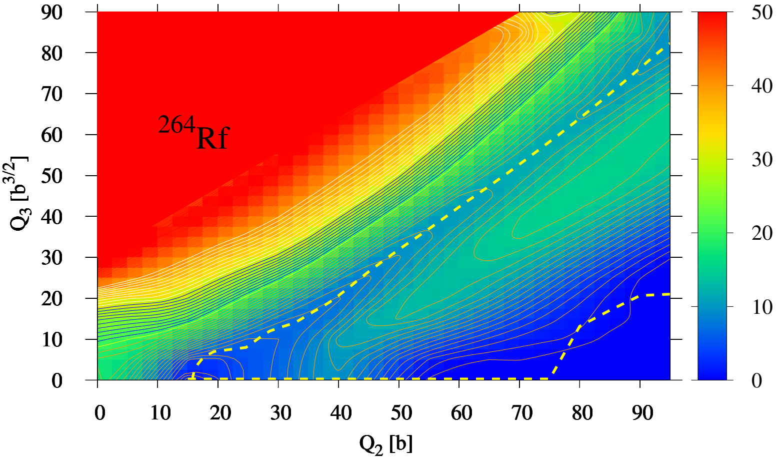

^{268}Sg

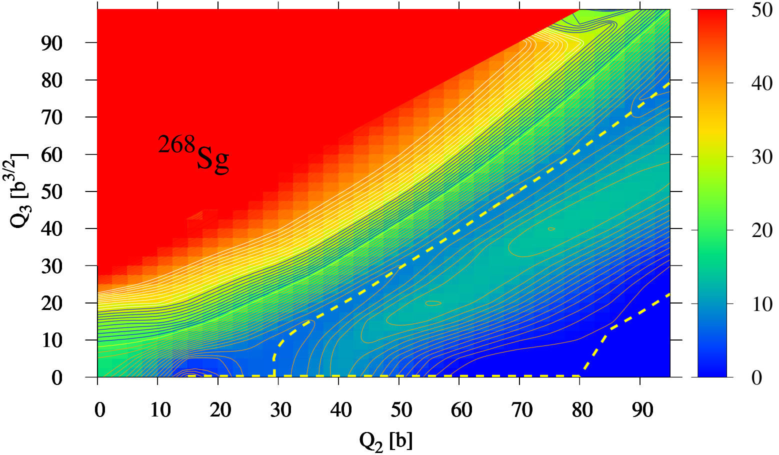

^{274}Hs

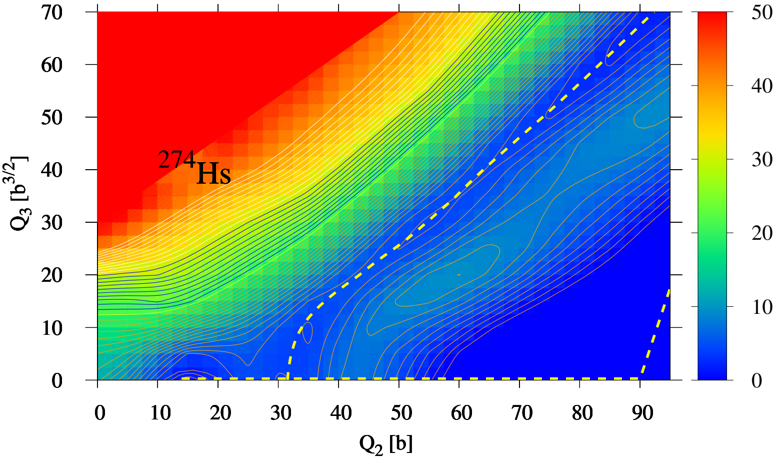

70
60
50
40
30
20
10
0
Q3 [b3/2]
274Hs
0
10
20
30
40
50
60
70
80
90
Q2 [b]
50
40
30
20
10
0

^{278}Ds

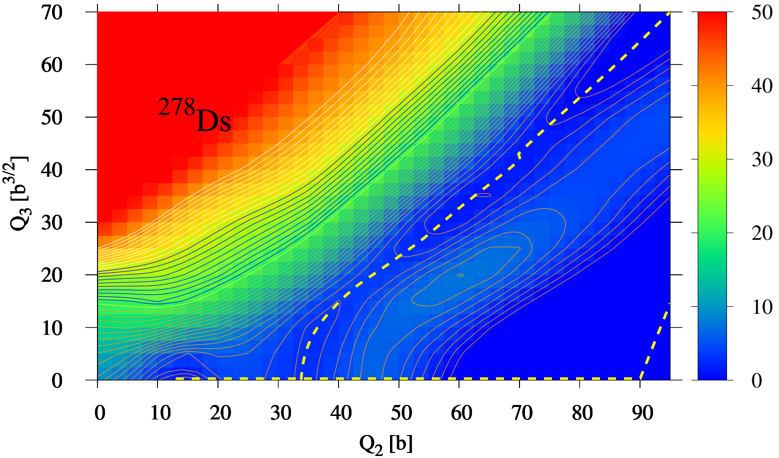

70
60
50
40
30
20
10
0
^{278}Ds
Q_3 [$b^{3/2}$]
0
10
20
30
40
50
60
70
80
90
Q_2 [b]
50
40
30
20
10
0

^{284}Cn

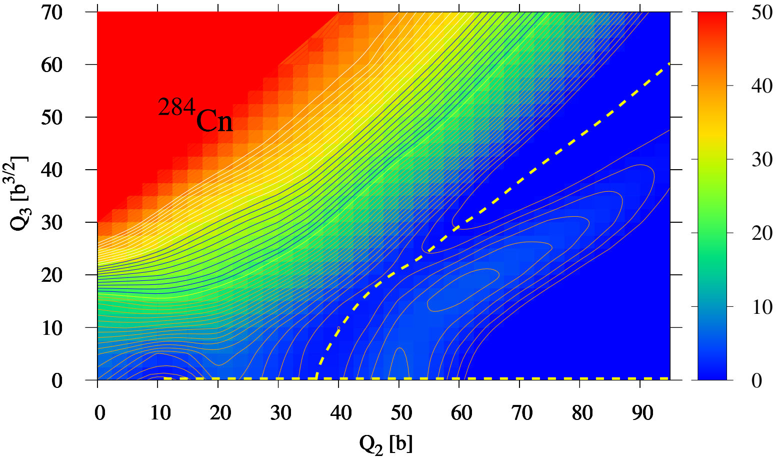

^{290}Fl

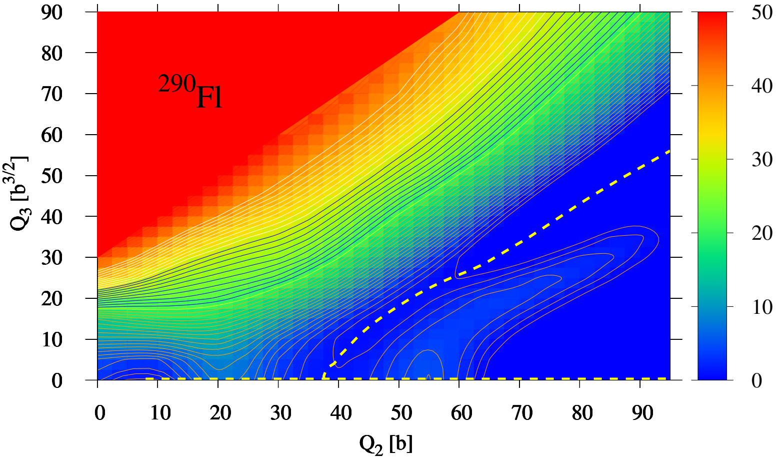

^{294}Lv

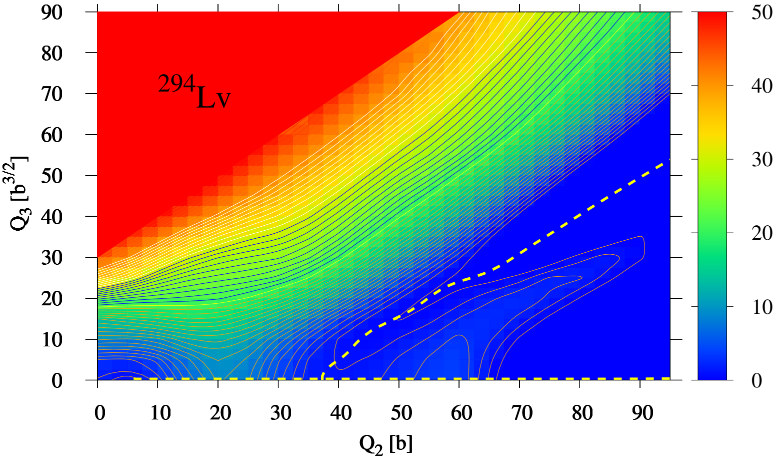

Cluster barriers

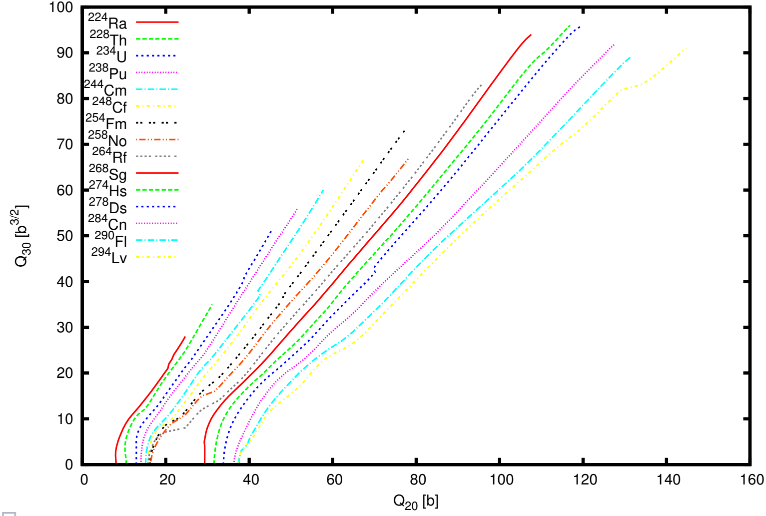

www.umcs.lublin.pl

Cluster barriers

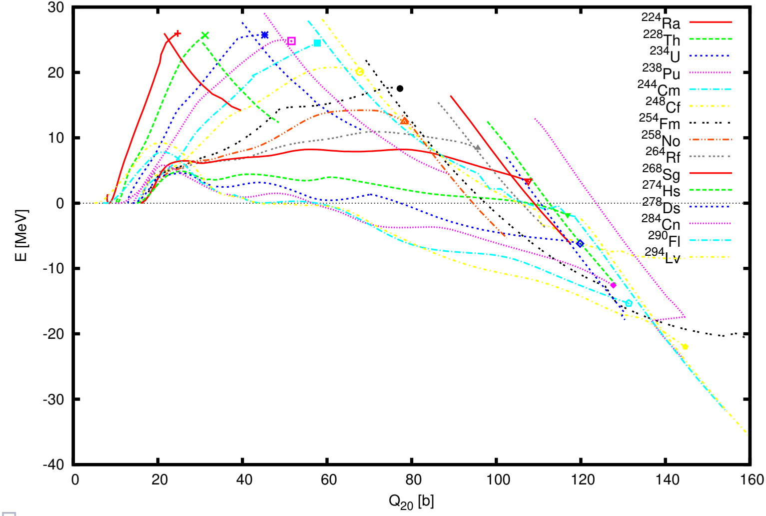

Cluster barriers

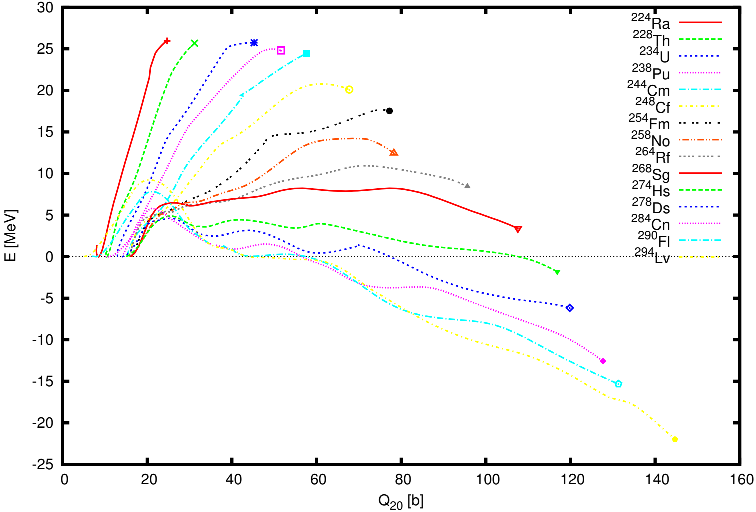

Pre-scission shapes

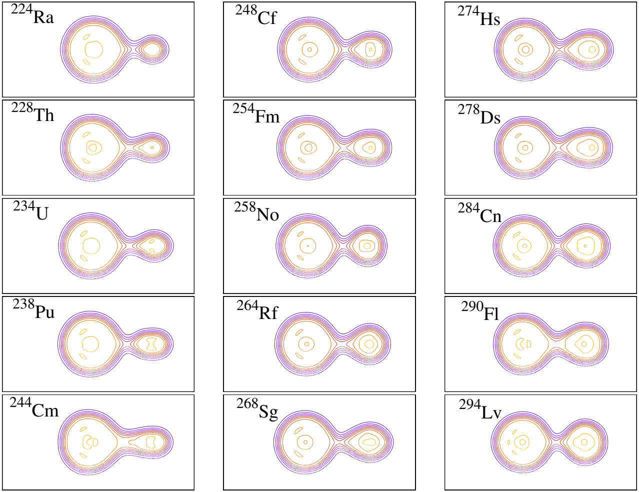

Post-scission shapes

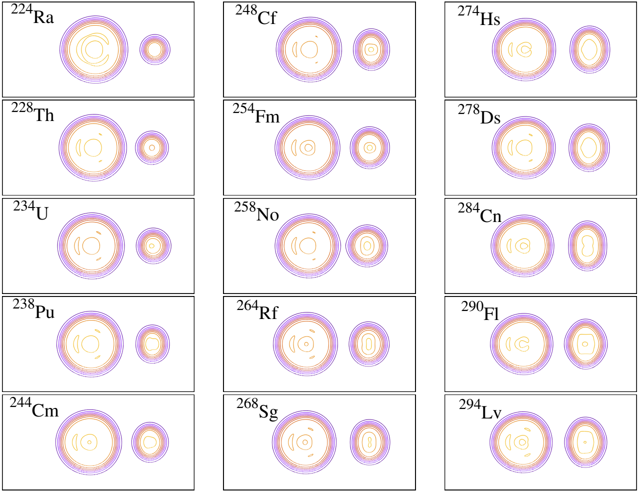

Cluster barriers

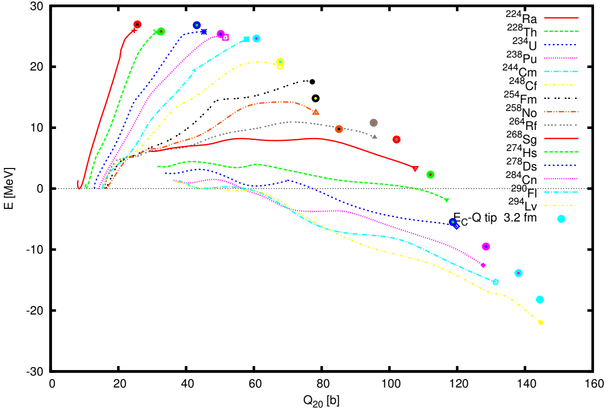

$$E = k\frac{82(Z-82)e^2}{r_{208}+r_{A-208}+d} - Q$$

Half-llives

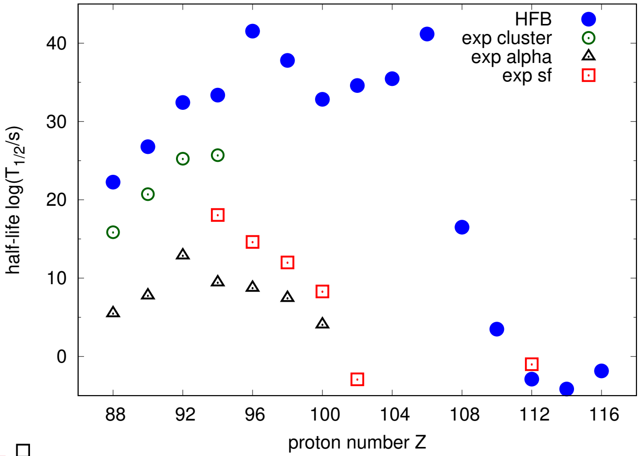
HFB
exp cluster
exp alpha
exp sf
40
30
20
10
0
half-life log($T_{1/2}$/s)
88
92
96
100
104
108
112
116
proton number Z

Experimental evidence in ^{284}Cn:

- GSI: 9 events
  Ch. Düllmann, at al., Phys.Rev.Lett. 104, 252701 (2010)
- Dubna: 19 events
  Yu. Oganessian, Radiochim.Acta 99, 429 (2011)
- lifetimes: 30 ms - 400 ms

^{284}Cn

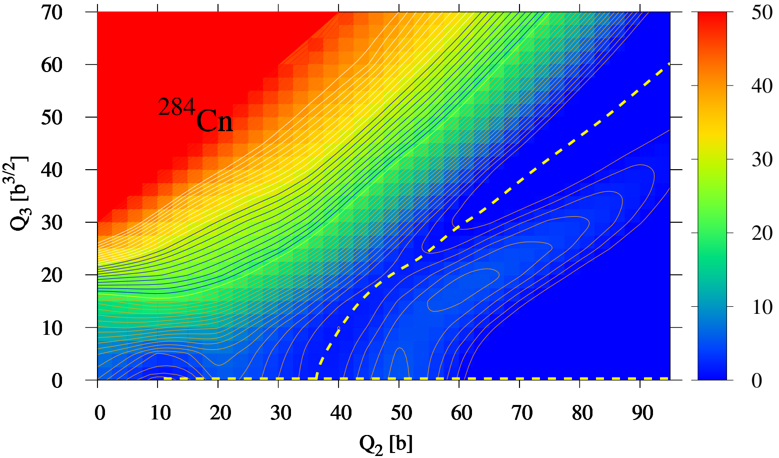

^{284}Cn
70
60
50
40
30
20
10
0
Q_3 [$b^{3/2}$]
0
10
20
30
40
50
60
70
80
90
Q_2 [b]
50
40
30
20
10
0

^{284}Cn

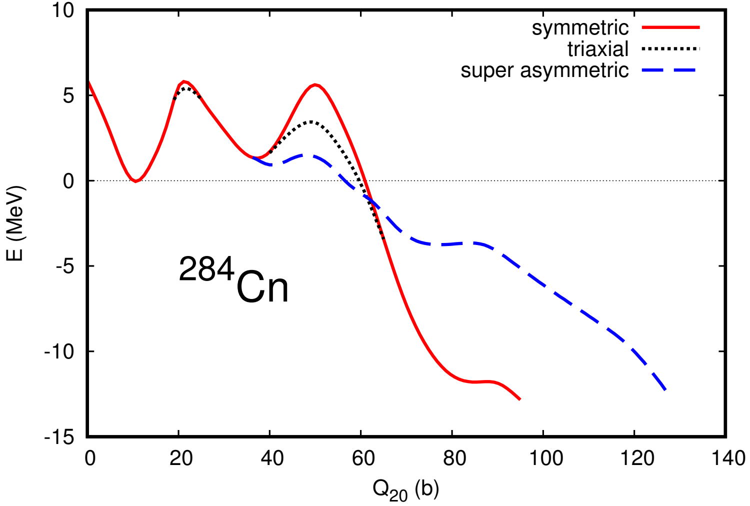
symmetric
triaxial
super asymmetric
E (MeV)
Q20 (b)
284Cn
10
5
0
-5
-10
-15
0
20
40
60
80
100
120
140

^{284}Cn

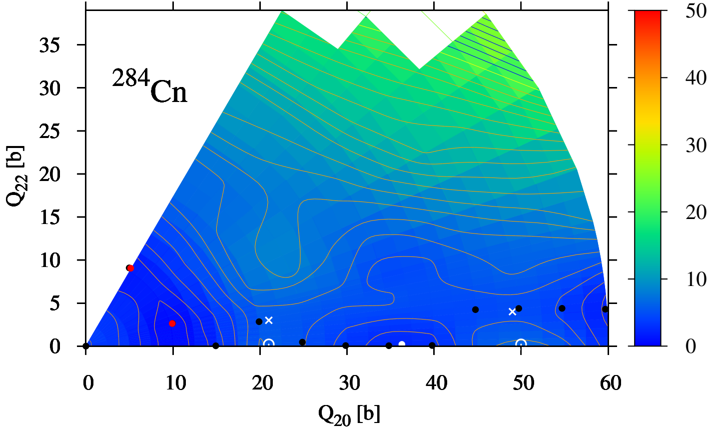

^{284}Cn
Q_{22} [b]
Q_{20} [b]
0
5
10
15
20
25
30
35
0
10
20
30
40
50
60
0
10
20
30
40
50

Chart of SH nuclides

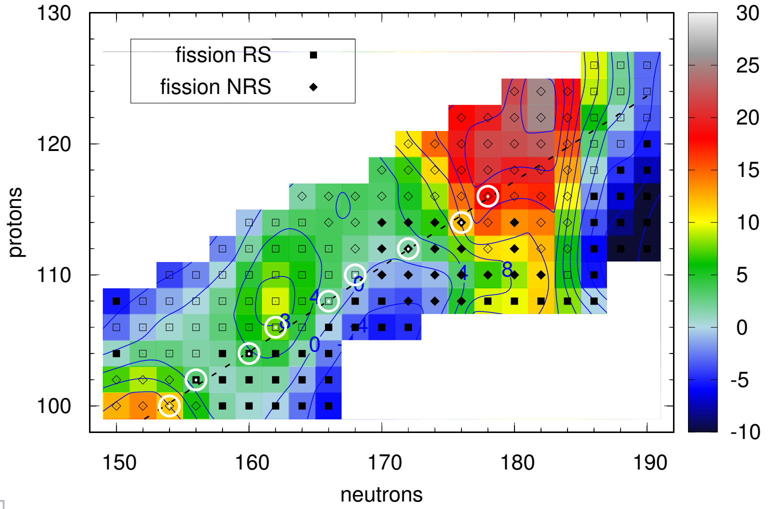

www.umcs.lublin.pl

Actinides and superheavies

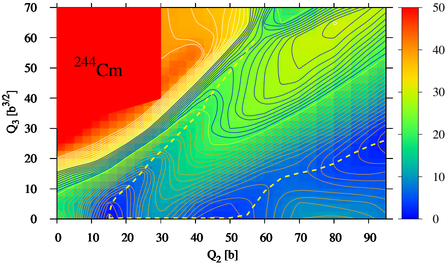

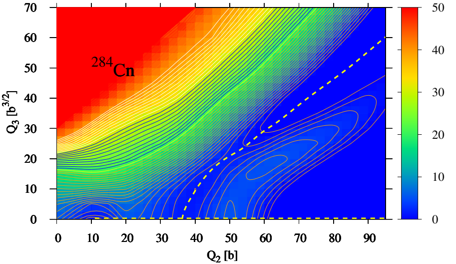

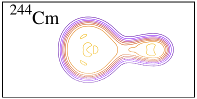

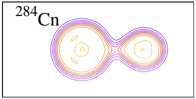

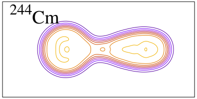

Fragment mass distribution - preliminary

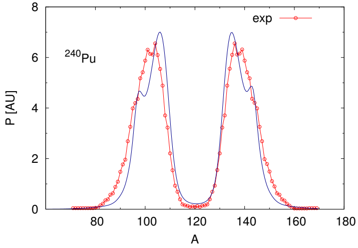

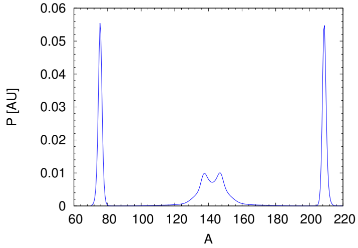

www.umcs.lublin.pl

Mean fission fragment mass

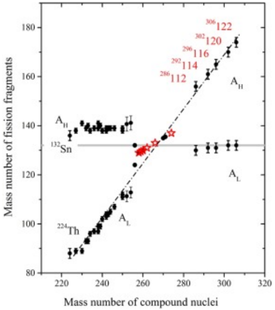

M.G.Itkis, E.Vardaci, I.M.Itkis, G.N.Knyazheva, E.M.Kozulin, Nuclear Physics A944 (2015) 204

Mean fission fragment mass

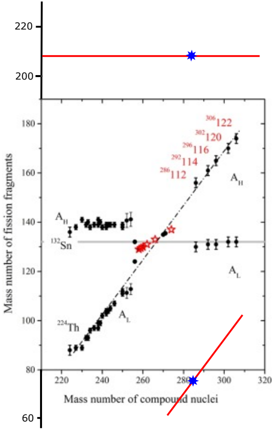

M.G.Itkis, E.Vardaci, I.M.Itkis, G.N.Knyazheva, E.M.Kozulin, Nuclear Physics A944 (2015) 204

Alternative predictions

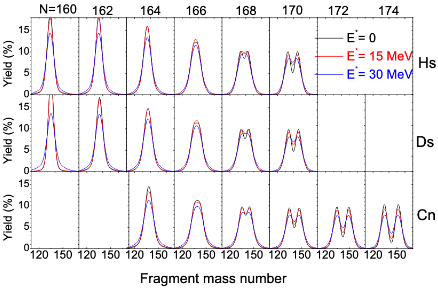

FIG. 3. The calculated fragment mass distributions for isotopes of Hs, Ds, and Cn for which spontaneous fission has been detected. Three values of the excitation energy E^* have been considered. $T_{\rm coll} = 2$ MeV, $E_d = 40$ MeV.

N. Carjan, F. A. Ivanyuk, and Yu. Ts. Oganessian Phys. Rev. C 99, 064606 (2019)

Conclusions

New type of fission is predicted:
super-asymmetric fission with ^{208}Pb as a heavy mass fragment

- the same nature as cluster radioactivity in actinides
- may be dominant in some super heavy nuclei
- sharp fragment mass distribution is predicted

Microscopic description of cluster radioactivity in actinide nuclei
M. Warda., L.M. Robledo
Physical Review **C 84** 044608 (2011)

Cluster Radioactivity in Super Heavy Nuclei
M. Warda, A. Zdeb, L.M. Robledo
Phys. Rev. **C 98** 041602(R) (2018)

Conclusions

New type of fission is predicted:
super-asymmetric fission with ^{208}Pb as a heavy mass fragment

- the same nature as cluster radioactivity in actinides
- may be dominant in some super heavy nuclei
- sharp fragment mass distribution is predicted

Microscopic description of cluster radioactivity in actinide nuclei
M. Warda., L.M. Robledo
Physical Review **C 84** 044608 (2011)

Cluster Radioactivity in Super Heavy Nuclei
M. Warda, A. Zdeb, L.M. Robledo
Phys. Rev. **C 98** 041602(R) (2018)

Conclusions

New type of fission is predicted:
super-asymmetric fission with ^{208}Pb as a heavy mass fragment

- the same nature as cluster radioactivity in actinides
- may be dominant in some super heavy nuclei
- sharp fragment mass distribution is predicted

Microscopic description of cluster radioactivity in actinide nuclei
M. Warda., L.M. Robledo
Physical Review **C 84** 044608 (2011)

Cluster Radioactivity in Super Heavy Nuclei
M. Warda, A. Zdeb, L.M. Robledo
Phys. Rev. **C 98** 041602(R) (2018)

Conclusions

New type of fission is predicted:
super-asymmetric fission with ^{208}Pb as a heavy mass fragment

- the same nature as cluster radioactivity in actinides
- may be dominant in some super heavy nuclei
- sharp fragment mass distribution is predicted

Microscopic description of cluster radioactivity in actinide nuclei
M. Warda., L.M. Robledo
Physical Review **C 84** 044608 (2011)

Cluster Radioactivity in Super Heavy Nuclei
M. Warda, A. Zdeb, L.M. Robledo
Phys. Rev. **C 98** 041602(R) (2018)

Conclusions

New type of fission is predicted:
super-asymmetric fission with ^{208}Pb as a heavy mass fragment

- the same nature as cluster radioactivity in actinides
- may be dominant in some super heavy nuclei
- sharp fragment mass distribution is predicted

Microscopic description of cluster radioactivity in actinide nuclei
M. Warda., L.M. Robledo
Physical Review **C 84** 044608 (2011)

Cluster Radioactivity in Super Heavy Nuclei
M. Warda, A. Zdeb, L.M. Robledo
Phys. Rev. **C 98** 041602(R) (2018)